Experimental Study of Shadow Region Imaging Algorithm with Multiple Scattered Waves for UWB Radars

Shouhei KIDERA†, Takuya SAKAMOTO‡ and Toru SATO‡
† Graduate School of Electro-Communications, University of Electro-Communications
‡ Graduate School of Informatics, Kyoto University

Abstract

Ultra-wide band (UWB) radar holds high range resolution in the near field sensing, and is thus applicable to security systems designed to identify a human body even in invisible situations. Although Synthetic Aperture Radar (SAR) creates a stable and accurate target image for such applications, it often suffers from increased shadow regions in the case of complex or multiple targets. On the contrarily, a multiple scattered wave has the potential to enlarge a visible range because it propagates a path, that differs from that of a single scattered wave. While various algorithms based on time-reversal processing with multiple scattered waves have been developed, these require a priori information of the surroundings or a target model. This paper proposes a shadow region imaging algorithm based on the aperture synthesis of multiple scattered waves, that can directly increase the visible area and is applicable to arbitrary target shapes. This algorithm reconstructs a target image by synthesizing a double scattered wave according to its propagation path. The results in numerical simulations and an experiment verifies the effectiveness of the proposed method that it directly makes a shadow region visible without a preliminary observation.

1 Introduction

UWB pulse radar is promising as a near field sensing technique with high range resolution, and is applicable to non-contact measurement of precision devices with specular surfaces, like reflector antennas or aircraft bodies that have high-precision and specular surfaces, or to spatial measurement for security systems and rescue robots that can identify a human body in invisible situations. There are various algorithms in suitable for these applications. The SEABED algorithm accomplishes a real-time imaging by using a reversible transform BST[1], Envelope+SOC remarkbaly enhances the image resolution less than 1/100 wavelength [2]. Also, the SAR algorithm is still promising, in terms of providing a stable and accurate image by using full information of received signals. However, in the case of complex or multiple targets, any of algorithms suffers from increased shadow regions as long as only the single scattered wave is used for imaging. On the contrarily, except for a edge diffraction wave, a multiple scattered wave propagates the path, that is different from that of a single scattered wave. This means that the multiple scattered echo has a significant information on target surfaces, and thus has the potential to improve the image quality of the conventional methods, which use only single scattered waves. Although some of the time reversal algorithms with multiple scattered waves have been proposed when focusing on a reliable target detection or accurate positioning in cluttered situations [3, 4, 5], they require a target modeling or a priori information of the surrounding environment like walls. To relax these restrictions, this paper proposes a direct imaging algorithm based on aperture synthesis of multiple scattered echoes. As a novelty of this paper, the proposed method is applicable to arbitrary target shapes, and directly enlarges the visible range on the target surface. Results obtained from numerical simulation and an experiment verify the effectiveness of the proposed method.

2 Conventional algorithm

Fig. 1 shows the system model. It assumes that the target has an arbitrary shape with a clear boundary, and high conductivity like metallic objects. The propagation speed of the radio wave c is assumed to be known constant. A mono-cycle pulse is used as the transmitting current. The antenna that has a linear polarization in the x direction, is scanned along the plane $z = 0$. The real space in which the target and antenna are located is expressed by the parameter $\boldsymbol{r} = (x, y, z)$. $z > 0$ is assumed for simplicity. $s(X, Y, Z')$ is defined as the output of the Wiener filter at the antenna location $(x, y, z) = (X, Y, 0)$.

As the spatial measurement for the near field, the SAR algorithm has an ability to create a stable and

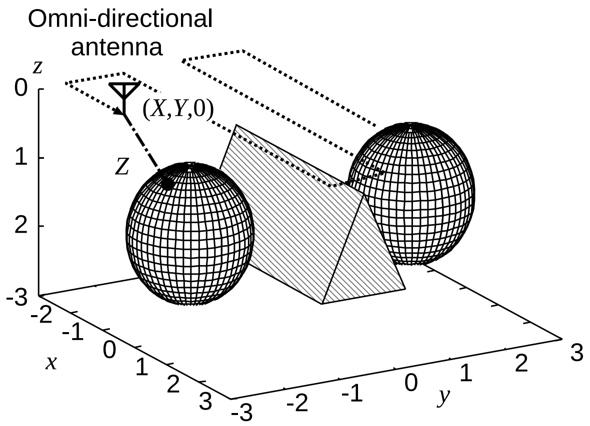

Figure 1: System model in 3-D problem.

accurate image by using UWB signal. The distribution image obtained by the SAR, $I_1(\boldsymbol{r})$ is formulated as

$$I_1(\boldsymbol{r}) = \int_{\boldsymbol{q}\in\Gamma} s\left(\boldsymbol{q}, d_1(\boldsymbol{r},\boldsymbol{q})/2\right) \mathrm{d}X\mathrm{d}Y \tag{1}$$

where $\boldsymbol{q} = (X, Y)$ and Γ is the scanning range of the antenna. $d_1(\boldsymbol{r},\boldsymbol{q})$ is the round-trip distance between the point $\boldsymbol{r}$ and the antenna location as $(X, Y, 0)$. The target boundary can be extracted from its focused image $I_1(\boldsymbol{r})$. This algorithm has an advantage that it can create the stable image for various target shape by using a full information of received signals $s(X, Y, Z)$. The example in the numerical simulation is presented as follows. The target shown in Fig. 1 is assumed. The received signals are observed for $-2.5 \leq X, Y \leq 2.5$ at 51 locations for each axis. The left hand side of Fig. 2 shows the image viewed at $x = 0$ with the conventional SAR, and it shows that the image expresses only the bottom part of the target boundary, and the most part of the triangular boundary falls into shadow regions. This is because each antenna does not receive a significant reflection echo from the side of the boundary with a large inclination. This is an inherent problem in imaging algorithms that only use single scattered echoes for target reconstruction.

3 Proposed Algorithm

To overcome the previous problem, this paper proposes a shadow region imaging algorithm based on the aperture synthesis of double scattered echoes. A double scattered wave propagates a different path from that of a single scattered one, except for an edge diffraction wave. Then it often provides a significant information of two reflection points on the target boundaries. The proposed method calculates the distribution image $I_2(\boldsymbol{r})$ synthesized by the double scattering data as

$$I_2(\boldsymbol{r}) = -\int_{\boldsymbol{q}\in\Gamma}\int_{\boldsymbol{r'}\in R} I_1(\boldsymbol{r'}) s\left(\boldsymbol{q}, d_2(\boldsymbol{r},\boldsymbol{r'},\boldsymbol{q})/2\right) F(\boldsymbol{r},\boldsymbol{r'}\boldsymbol{q}) \quad \mathrm{d}x'\mathrm{d}y'\mathrm{d}z'\mathrm{d}X\mathrm{d}Y$$

where $\boldsymbol{r'} = (x', z')$, R denotes the region of the real space. $d_2\left(\boldsymbol{r},\boldsymbol{r'},\boldsymbol{q}\right)$ is the peripheral distance of the triangle whose apexes are $\boldsymbol{r}$, $\boldsymbol{r'}$ and the antenna location. The weighting function $F(\boldsymbol{r},\boldsymbol{r'},\boldsymbol{q})$ is defined as

$$F(\boldsymbol{r},\boldsymbol{r'}\boldsymbol{q}) = 1 - \exp\left[-\frac{\{d_2(\boldsymbol{r},\boldsymbol{r'},\boldsymbol{q}) - 2d_1(\boldsymbol{r},\boldsymbol{q})\}^2}{2\sigma_{\mathrm{FZ}}^2}\right], \tag{2}$$

where σ_{FZ} is determined empirically. $F(\boldsymbol{r},\boldsymbol{r'},\boldsymbol{q})$ suppress the weight for the region included in the Fresnel zone, determined by the initial image $I_1(\boldsymbol{r})$. The minus sign in Eq. (2) creates a positive image focused by double scattered waves, that have an inverse phase relationship from that of single scattered wave. Eq.(2) expresses the aperture synthesis of the received signals by only considering a double scattered path.

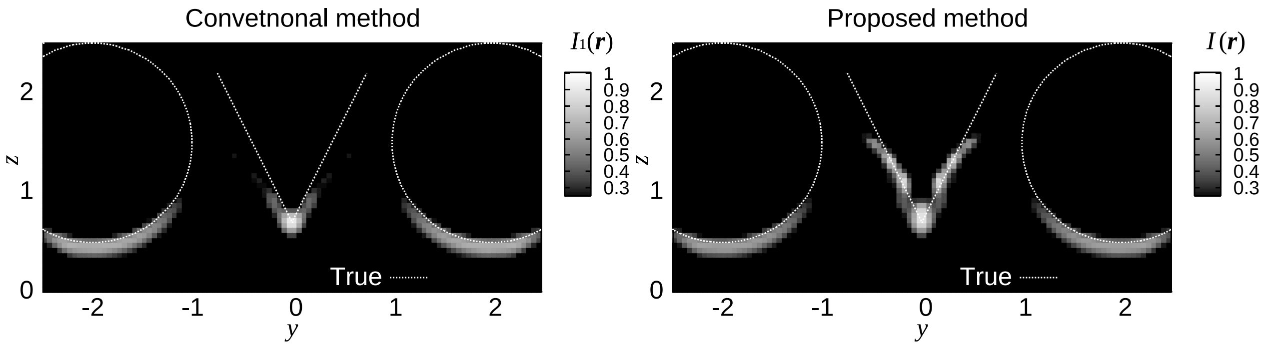

Figure 2: Estimated images with the conventional (left) and the proposed method (right).

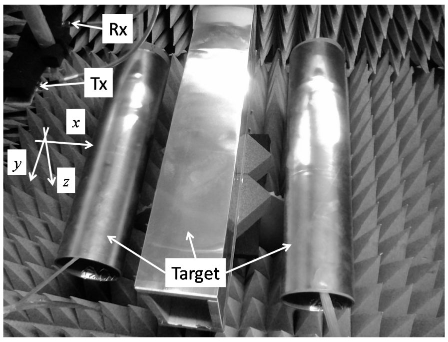

Figure 3: Arrangement of the antenna and the multiple targets in the experiment.

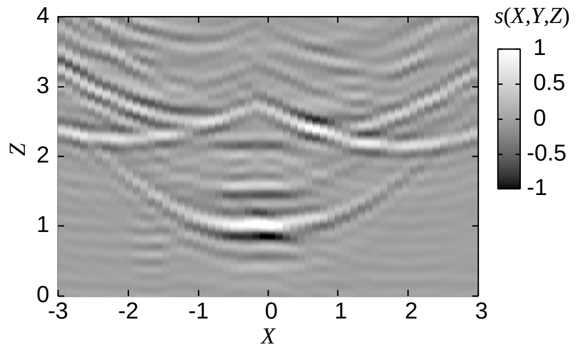

Figure 4: Output of Wiener filter in the experiment at $Y = 0$.

Here, we assume that only the positive images of $I_1(\boldsymbol{r})$ and $I_2(\boldsymbol{r})$ are necessary for the target boundary extraction. Then, the proposed method determines the final image $I(\boldsymbol{r})$ as,

$$I(\boldsymbol{r}) = I_1(\boldsymbol{r})H(I_1(\boldsymbol{r})) + I_2(\boldsymbol{r})H(I_2(\boldsymbol{r})) \tag{3}$$

The proposed method uses only the initial image $I_1(\boldsymbol{r})$ and directly emphasizes the target regions, where double scattered waves pass through. The right hand side of Fig. 2 shows the example of the proposed method viewed at $y = 0$, when the same data in the left side hand of Fig. 2 is used. This result reveals that the proposed method makes the shadow region visible, including the side of the triangle shape. This is because the double scattered waves are effectively focused on the rectangular side in Eq. (2). The reconstructible region provides us a indispensable image to identify the target shape.

4 Performance Evaluation in Experiment

This section shows the experimental investigation of the proposed algorithm. Fig. 3 shows the experimental setup with both cylindrical and rectangular targets. The UWB pulse with a 10 dB-bandwidth of 2.0 GHz and a center wavelength λ of 93.75 mm is used. The pair of the transmitting and receiving antennas is scanned on the $z = 0$ plane, for $-3.0\ \lambda \leq x \leq 3.0\lambda$ and $-1.0\lambda \leq y \leq 1.0\lambda$, respectively, with both sampling intervals set to 0.1λ. The antenna has an elliptic polarization, and the major polarimetric axis is along the y-axis. The data are coherently averaged 1024 times. The direct scattered signal from the trapezoidal target can be obtained by eliminating the reflection signal without a target.

Fig. 4 shows the output of Wiener filter at $Y = 0$ in the experiment. The S/N of the double scattered wave is around 25 dB. At the range for $2.5\lambda \leq Z \leq 3.0\lambda$, we can recognize the double scattered wave which has a inverse phase of the single one. The left hand side of Fig. 5 shows the estimated image at $y = 0$ with the conventional method. This figure shows that the only the bottom part of the target boundary is reconstructed.

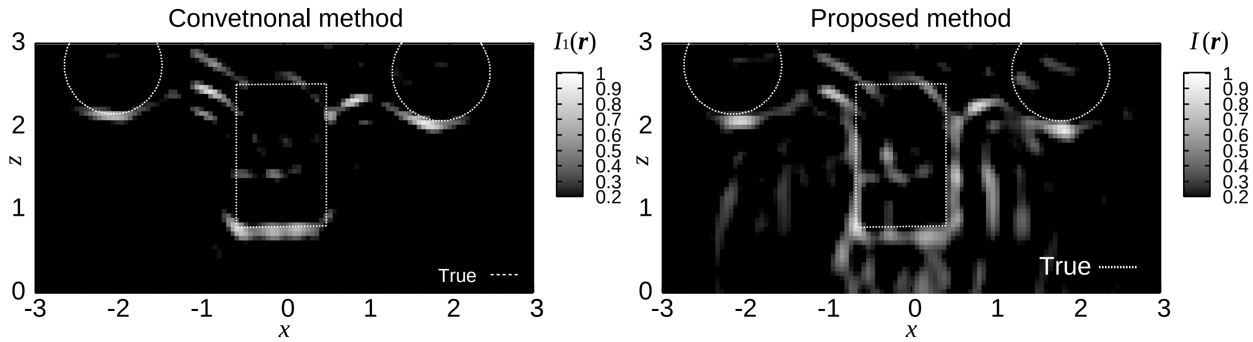

Figure 5: Estimated images with the conventional method (left) and proposed method (right) in the experiment ($y = 0$).

Contrarily, the right hand side of Fig. 5 shows the estimated image with the proposed method. Here, the bi-static extension of the proposed method is applied. The obtained image reconstucts the side of the rectangular target, and expands the visible area of the target boundary, since the double scattered waves are focused on this region. This result verifies that the proposed method effectively enlarges the visible area on target surfaces even in a real environment. Moreover, it is noteworthy that this method does not require a target modeling or a priori information of the surroundings, and yet it is a significant improvement from the conventional works [5]. However, the calculation time for a cross-section image is required around 100 minutes with a single Xeon 2.8 GHz processor, Thus, an acceleration of the imaging speed is also required in our future work.

5 Conclusion

This paper proposed the direct shadow region imaging algorithm based on aperture synthesis for double scattered waves. In the conventional SAR using only a single scattered echo, the greater part of a complex target or multiple targets falls into a shadow region. To overcome this problem, we extended the SAR algorithm to use double scattered waves. The advantage of the proposed method is that it does not require the priori information of the surroundings and object shape. The results from numerical simulation and experiment verified that the proposed algorithm can enhance the visible region and offers a significant target image even in a real environment. Although the proposed method requires a great deal of calculation, it has the potential to expand the application range of near field radar in cluttered situations.

References

[1] T. Sakamoto, *IEICE Trans. Commun.*, vol.E90-B, no.3, pp. 636–644, 2007.

[2] S. Kidera, T. Sakamoto and T. Sato, *IEEE Trans. Geosci. Remote Sens.*, vol. 46, no. 11, Oct., 2008.

[3] S. K. Lehmanm and A. J. Devaney, *Acoust. Soc. Am.,* 113 (5), May, 2003.

[4] J. M. F. Moura, and Y. Jin, *IEEE Trans. on Signal Process.*, vol. 55, no. 1, pp. 187–201, Jan, 2007.

[5] T. Kitamura, T. Sakamoto and T. Sato, *IEICE General Conference*, C-1-9, Mar, 2008 (in Japanese).